Flame propagation visualization in a spark-ignition engine using laser-induced fluorescence of cool-flame species

Bladh, Henrik; Brackmann, C; Dahlander, P; Denbratt, I; Bengtsson, Per-Erik

Published in:
Measurement Science & Technology

DOI:
10.1088/0957-0233/16/5/006

2005

INSTITUTE OF PHYSICS PUBLISHING MEASUREMENT SCIENCE AND TECHNOLOGY

Meas. Sci. Technol. **16** (2005) 1083–1091 doi:10.1088/0957-0233/16/5/006

Flame propagation visualization in a spark-ignition engine using laser-induced fluorescence of cool-flame species

H Bladh[1], C Brackmann[1], P Dahlander[2], I Denbratt[2] and P-E Bengtsson[1]

[1] Division of Combustion Physics, Lund Institute of Technology, PO Box 118, SE-221 00 Lund, Sweden

[2] Thermo and Fluid Dynamics, Chalmers University of Technology, SE-41296 Gothenburg, Sweden

E-mail: Henrik.Bladh@forbrf.lth.se

Received 8 October 2004, in final form 10 January 2005
Published 22 March 2005
Online at stacks.iop.org/MST/16/1083

Abstract

The flame propagation in a spark-ignition engine has been studied using laser-induced fluorescence (LIF) of species formed during the first ignition stage of hydrocarbon combustion. The detected two-dimensional LIF images showed the distribution of unburned regions. For the excitation, two Nd:YAG lasers operating at 355 nm were used for two consecutive measurements within the same engine cycle with adjustable time separation between the pulses. Two ICCD cameras that were synchronized to each of the laser pulses recorded pairs of fluorescence images, i.e. the movement of the flame front could be tracked. It is well known that formaldehyde is excited using a wavelength of 355 nm and a spectral signature of this species was also identified in engine LIF spectra. Programme routines were developed and used for evaluation of the flame propagation velocity from the fluorescence images. This paper presents the potential and the characteristics of the experimental technique as well as the evaluation procedure. The measurements of cool-flame intermediates have also been compared with measurements of fuel-tracer as an indicator of unburned fuel–air mixture. A good agreement between position and shape of the signal areas was obtained at crank angles where both fluorescence signal from cool-flame species excited at 355 nm and added 3-pentanone excited at 266 nm could be detected.

Keywords: combustion diagnostics, laser-induced fluorescence, spark-ignition engine, flame propagation

1. Introduction

Optical methods have for a long time been useful tools for experimental investigations of combustion in internal combustion engines, and especially the use of laser-based diagnostic methods has during the last decades made measurements of species, temperature, gas flow, droplets and particles possible with high spatial as well as temporal resolution. Among the laser-based methods, laser-induced fluorescence (LIF) has been widely used for species detection [1–3]. The method is species specific for smaller molecules and two favourable characteristics of the technique are the possibilities of detecting species of low concentration, such as combustion intermediates, and of performing two-dimensional imaging measurements. The method also has limitations, for instance the species selectivity is partly lost with increasing molecular size for molecules such as aldehydes, ketones and polyaromatic hydrocarbons with broad featureless absorption and fluorescence spectra. Moreover, the fluorescence yield is dependent on local conditions such as temperature, pressure

and composition, which makes quantitative measurements difficult.

The oxidation of many hydrocarbon fuels, such as the mixture of n-heptane and iso-octane used in the present study, occurs through a two-stage ignition process [4]. In the first stage, intermediate species such as formaldehyde are produced in the cool-flame chemistry. These intermediates are then consumed during the second stage in the continuing combustion chemistry. Hence, the presence of cool-flame species such as formaldehyde indicates the onset of hydrocarbon oxidation in the unburned fuel–oxidant mixture. The detection of formaldehyde by laser-induced fluorescence has been performed in flames [5–8] as well as in internal combustion engines [9–15]. The absorption bands of formaldehyde exist from the near UV region to down below 300 nm [16–19]. One convenient possibility from an experimental point of view is to use the third harmonic of a conventional Nd:YAG laser at the wavelength of 355 nm for the excitation of formaldehyde [20]. This is the alternative that has been used in the present work. Although this wavelength does not overlap with the strongest molecular transitions, single-shot images with relatively high signal-to-noise ratio have been obtained in engines [12, 13, 20]. However, it is important to note that the fluorescence signal obtained in engine measurements using excitation at 355 nm may not solely be due to formaldehyde. Other intermediates are formed at the first ignition stage and may give spectral fluorescence contributions.

Normally, a laser-induced fluorescence experiment is based on a pulsed laser having a repetition rate of tens of Hz. This means that only one measurement can be performed per cycle for engines run at a few thousand revolutions per minute. One possibility of performing two measurements within an engine cycle is to use a laser system which can be operated in double-pulse mode, but this alternative has limitations concerning the time separation that can be obtained with adequate pulse energy. Hence, laser-based cycle-resolved studies generally require the use of setups with multiple lasers and detectors. Engine measurements on combustion intermediates using dual lasers and detectors have been presented in several papers [10, 14, 15]. These measurements were performed in a two-stroke research engine with a side-valve configuration and optical access from the top. This configuration provided optical access to the entire combustion chamber and enabled studies of phenomena occurring near the walls, in this case the development of exothermic centres, which may lead to the phenomenon of engine knock.

In contrast to those studies, the present work was carried out with a more realistic engine geometry consisting of a pent-roof top with four valves and a centred spark plug. The experimental setup consisted of two Nd:YAG lasers with an adjustable time separation between the pulses, and two ICCD cameras, each synchronized with one of the lasers. This setup made it possible to detect two images of the spatial distribution of cool-flame intermediates within the same engine cycle, from which the flame propagation could be evaluated. The paper presents and discusses the experimental procedure together with the image analysis.

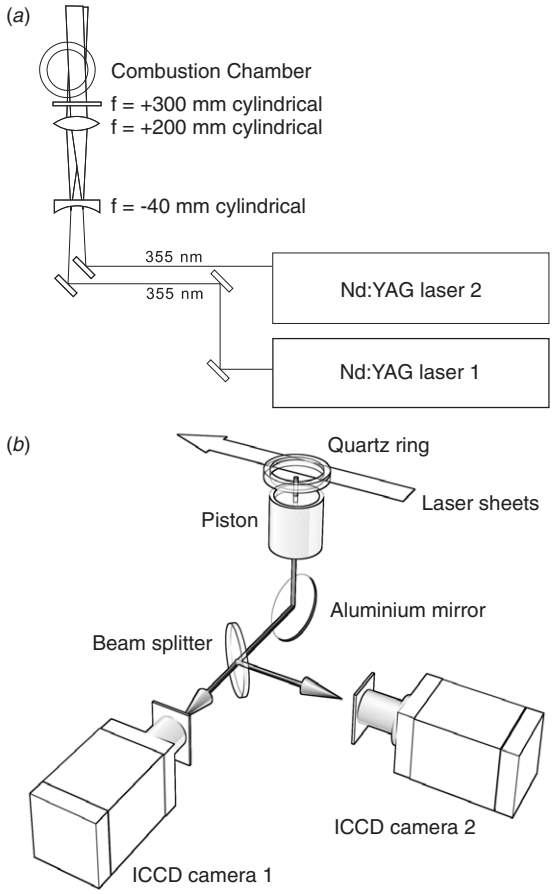

Figure 1. (*a*) The laser beam arrangement in the experimental setup. The two Nd:YAG laser sheets at the wavelength 355 nm entered and exited the combustion chamber through a quartz ring inserted as a part of the cylinder liner. (*b*) Detection setup, where the fluorescence signal was collected through the piston via the mirror onto the two detectors by use of a beam splitter.

2. Experimental details

The measurements presented in this study were all performed in a port-injected AVL 5411 single-cylinder research engine operated with a compression ratio of 8.5. The bore was 83 mm and the stroke 90 mm, resulting in a swept volume of 487 cm^3. The engine top was a VOLVO B5244 with a pent-roof geometry, equipped with four valves and the spark plug located at the centre of the pent-roof. Optical access to the combustion chamber was provided through windows in the pent-roof top, through a quartz ring in the upper part of the cylinder liner, and through a window in the flat piston. The fuel consisted of a mixture of n-heptane and iso-octane at a research octane number (RON) of 60, i.e. 60% iso-octane and 40% n-heptane. The inlet pressure was 2.7 bar and the inlet temperature was 30 °C for all cases if not stated otherwise. The engine was run at a constant speed of 1200 rpm, which is synchronized with the 10 Hz repetition rate of the lasers. The engine pressure was registered with a water-cooled pressure transducer mounted in the pent-roof. Parts of the engine and the setup are depicted in figure 1.

The wavelength 355 nm from two Nd:YAG lasers (Spectra Physics Quanta-Ray Lab 170/10 2000L and Quantel YG781C) was used for the LIF experiments. The laser

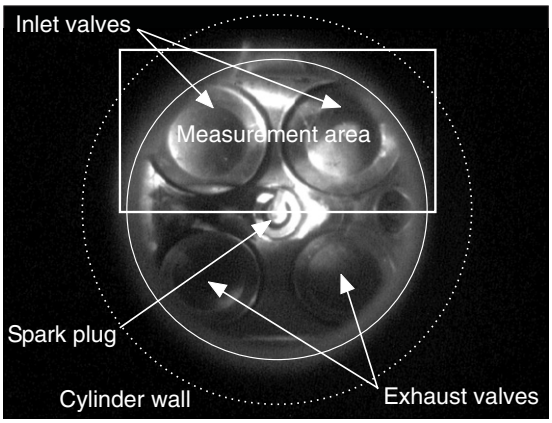

Figure 2. The view through the piston as viewed by the ICCD cameras. The inner circle indicates the boundary of the viewable area and the LIF measurement region is indicated by the rectangle.

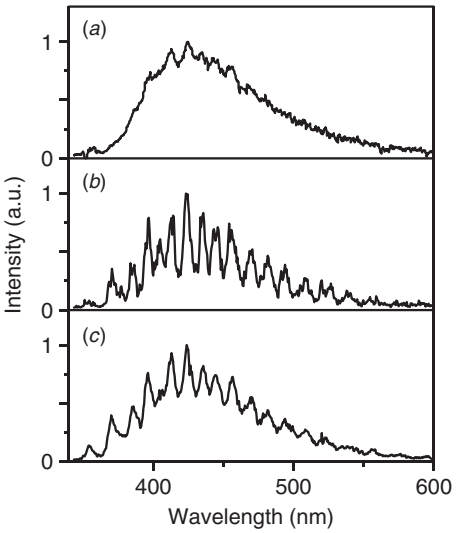

Figure 3. Laser-induced fluorescence spectra after excitation at 355 nm. (*a*) Obtained in the engine at −3 CAD, (*b*) obtained in a cell with formaldehyde vapour at 420 K and 5 bar, and (*c*) obtained in the cell at 770 K and 5 bar.

beams entered the combustion chamber through the quartz ring inserted as a part of the cylinder liner. The fluorescence was detected through the window in the piston and the observable area was 65 mm in diameter. The difference between this and the bore of 83 mm is due to the steel wall of the piston, which limits the view. The view through the piston is shown in figure 2, where the rectangle indicates the area corresponding to the LIF images presented in this paper. An aluminium mirror located below the piston reflected the fluorescence signal onto a beam splitter, which in turn divided it into two separate ICCD cameras (LaVision Flamestar II). The cameras had 14 bit resolution and CCD chips consisting of 384 × 576 pixels.

The laser beams were aligned in separate optical paths that overlapped inside the combustion chamber, as illustrated in figure 1(*a*). This arrangement was made to circumvent a reduction in pulse energy in each beam, which would result if the beams were aligned into one single path using dichroic beamsplitters. The small angle of incidence that was used (∼0.9°) caused the measurement volumes to be marginally different for the two laser beams. This was not considered a problem since it only affected the position of the edges of the laser sheets by a few mm.

The engine crank angle meter triggered two pulse generators (Stanford DG535), which in turn triggered the lasers and the ICCD cameras. The setup with two separate Nd:YAG lasers allowed for the time separation between the pulses from the two lasers to be set arbitrarily. The ICCD cameras could not operate at the 10 Hz repetition rate of the lasers and were limited to a rate of approximately 1 Hz.

Two initial experimental investigations were performed, a spectral investigation of the fluorescence and a measurement to determine the location inside the combustion chamber where the fluorescence most likely occurred. The spectral investigation was performed using a spherical lens of $f =$ 100 mm to collect the fluorescence to the slit of an $f =$ 150 mm Acton Research spectrometer equipped with a grating with 300 grooves mm^{-1}. In figure 3 an accumulated LIF spectrum is shown from the engine measurements (*a*) together with two LIF spectra from measurements on formaldehyde in a cell ((*b*) and (*c*)) previously presented by Metz *et al* [21]. The cell spectra were measured at a pressure of 5 bar and the temperatures were 420 K (*b*) and 770 K (*c*). For the accumulated engine spectrum the mean pressure was 25 bar. The engine spectrum is less resolved than the cell spectra, but nevertheless small peaks can be identified in the engine spectrum at spectral positions, which correspond well to those of the formaldehyde cell spectra. This indicates that formaldehyde is a major contributor to the LIF signal, but from the appearance of the engine spectrum contributions from other species cannot be excluded. A comparison between the spectra in figures 3(*b*) and (*c*) indicates that the spectral resolution of the formaldehyde peaks is partly lost with increasing temperature. This effect together with the elevated pressure in the engine, possible fluorescence from other species and the spectrometer slit function may account for the less resolved engine spectrum. It is well known that formaldehyde is excited at 355 nm [20], and since formaldehyde can be identified as a part of the detected LIF signal we will further on refer to this signal as the formaldehyde signal.

To identify the region in the combustion chamber where the formaldehyde signal was most likely to appear, measurements were performed using a laser sheet of ∼7.5 cm covering the whole cylinder cross section. The whole view through the piston window was imaged using a Nikon $f =$ 50 mm camera lens. It was concluded that the LIF signal was mainly located in the region of the measurement volume closest to the inlet ports. This corresponds to the indicated upper half of the viewable area depicted in figure 2. The presence of the signal in this region can be explained by the tumbling fluid motion within the combustion chamber, which convects the flame towards the exhaust valves, resulting in an end-gas region mainly located on the opposite side, near the inlet valves. Following these results it was possible to use laser sheets, approximately 4 cm wide, covering only the indicated region in figure 2. Concentrating the laser sheets onto this region ensured higher power densities in the probe volume resulting in higher signal-to-noise ratios in the images. The laser pulse energies were ∼50 mJ. At such high energies, laser-induced photo-chemistry may cause

the laser pulse in the first measurement to influence the result of the second. To establish if this phenomenon was present for the chosen pulse energies, engine measurements were carried out with a time separation between the laser pulses of 3 μs only, corresponding to 0.02 crank angles at 1200 rpm. This time separation was chosen long enough to isolate the laser pulses from each other, and still short enough for the measurements to be considered as simultaneous compared to the time-scale of the engine combustion cycle, i.e. the measurements were considered quasi-simultaneous. The image pairs captured during these measurements showed similar signal distributions, which indicates that laser-induced photo-chemistry was not an issue.

The smaller region of interest also made it possible to achieve a higher magnification in the images using Nikon $f = 105$ mm objectives. By focusing on a grid pattern placed on the top of the quartz glass of the piston, the ICCD cameras and the beam splitter could be aligned spatially to obtain pixel-to-pixel correspondence. The use of a grid also provided a scale for determination of the spatial resolution, which was estimated to be 120 μm/pixel. Long-pass filters (Schott GG385) were used to suppress scattered radiation at the laser wavelength and the gate widths of the ICCD cameras were set to 50 ns to suppress continuous background.

During engine operation the temperature of the cylinder wall and the piston increases, causing thermal stress on the optical parts. The AVL engine could therefore not be operated continuously longer than approximately half a minute. This made it impossible to reach steady-state operation and all measurements were performed in several series, each during a short time interval. In every measurement series 20 image pairs were captured together with the pressure traces for the same engine cycles.

In addition, a comparative study with fluorescence from nascent formaldehyde (excited at 355 nm) and fluorescence from the fuel tracer 3-pentanone was performed. For this purpose the RON 60 fuel was doped with 6% 3-pentanone on a volume basis and the tracer was excited using the wavelength 266 nm from one of the Nd:YAG lasers. The laser sheet widths were set to $\sim$2 cm to further enhance the power densities in the probe volume, and the pulse energies were $\sim$40 mJ in both beams. These measurements were made with the 3 μs time separation between the pulses previously described as quasi-simultaneous. The intention of these measurements was to establish that fluorescence in both cases originated from the same areas and to compare the techniques as markers for the unburned fuel region.

3. Image evaluation procedure

The data evaluation followed the scheme depicted in figure 4 and an example of a formaldehyde LIF image that was analysed is shown in figure 5. In this image both the signal region corresponding to the unburned gas region and the dark region corresponding to the burned gas region are clearly shown. The laser light is entering from the right in the picture, and streaks can be observed in the signal area in the left part of the image. Such streaks are caused by spatial redistribution of the intensity in the laser sheet due to density gradients in the flame front, and have previously been presented, for example in [14].

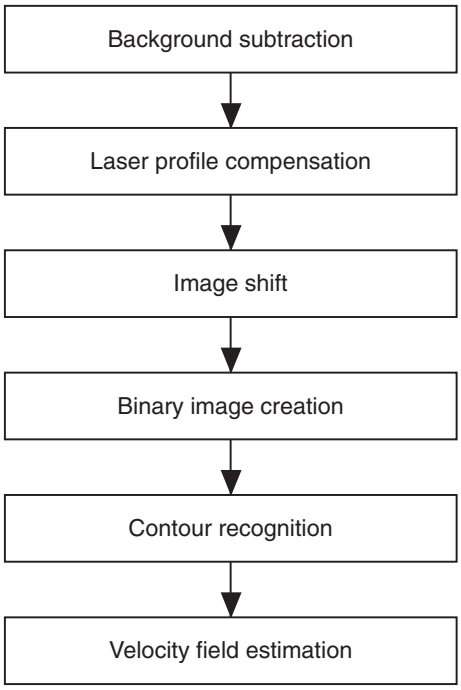

Figure 4. Chart illustrating the steps of the data evaluation procedure.

Figure 5. Formaldehyde LIF image obtained at -2 CAD in the engine showing the unburned gas region in the engine. A signal area can be seen located in the vicinity of the inlet valves (see figure 2).

Together with each set of image pairs taken during a measurement series, background images were collected running the engine motored. These background images did always, but to a varying degree, contain incandescence and fluorescence from deposits and oil on the engine ceiling and windows. To be able to compensate for the spatial intensity distribution in the laser sheets, LIF measurements were performed on fluorescing dye in a cuvette. The cuvette was positioned on the top of the optical piston at the location of the laser sheets, with the engine top removed. In this way both the sheet-forming optics and the detection setup were in the same position as during the engine measurements. During evaluation the images obtained from the fluorescing dye were used to extract intensity profiles across the laser sheets and the images from the engine measurements were later compensated by dividing them with these profiles. Since the profile measurements and the engine measurements were not carried out simultaneously, potential variations of the laser

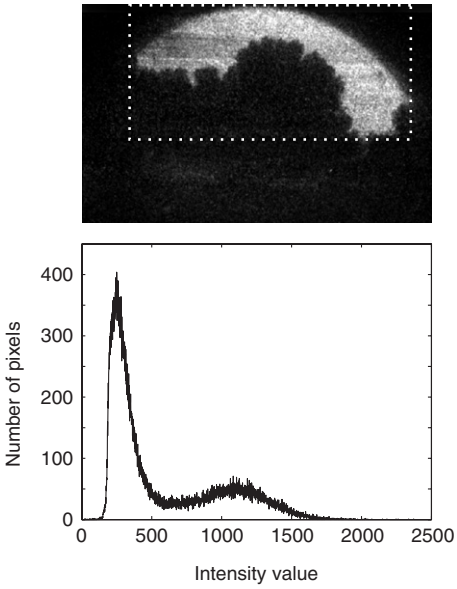

Figure 6. The intensity level histogram (below) of the marked area in the LIF image (above). The x-values correspond to certain discrete intensity values, and the y-values correspond to the number of pixels in the image that have this intensity value.

profile during the measurement series, or indeed fluctuations between individual pulses could not be accounted for. The first steps of the image evaluation included background subtraction, laser profile compensation and if necessary also image shift due to slightly misaligned cameras.

The evaluation of the flame propagation velocity requires identification of the contours of the signal areas in the two formaldehyde images. The first step in this procedure was to create binary images by selecting a threshold value on the intensity scales of the original images. To set a threshold value for an arbitrary image is generally not a problem if the signal-to-noise ratio is sufficiently high. However, it is not possible to use the same absolute threshold value for both images of a pair. This is because of the inherent signal level differences occurring as a result of using different lasers, detectors and signal collection optics. A relative threshold must therefore be used, related to the signal intensity values of each image. Setting the threshold as a fraction of the maximum intensity of an image may result in errors for the cases when the maximum does not arise from the formaldehyde signal. For example, some images show very bright spots, probably due to scattering and fluorescence from contaminating species such as droplets or particles. To handle the problems described above a more detailed treatment of the image intensity distribution using histograms was developed.

In figure 6, the intensity distribution of parts of the image presented in figure 5 is shown in a histogram. It shows the number of pixels having a certain intensity value and two groups of pixel intensities can be identified. The first and most prominent group can be found at intensities of a few hundred counts and corresponds to a low background level obtained in the burned region and from pixels located outside the field of view. The second group can be found at higher intensities typically around 1000 counts and corresponds to the LIF signal from the unburned region. The threshold value is set relative to the signal intensity distribution of this second group in the histogram. The criteria used for threshold determination were set using empirical studies and depending on the choice of parameters for the routine, somewhat different threshold values are obtained. Once set, these parameters were kept constant during the whole image evaluation process. The threshold values were used to create binary images from the images obtained from the first evaluation steps. The binary images were then processed with a program, which extracted the points on the contours. From a starting point on the contour this program examines neighbouring pixels, identifies the gradient and traces the contour until an end point is reached. In figures 7(a) and (b) an example of such identified contours is shown together with the two original images from the same engine cycle.

The two contours determined with this method can be used to estimate the flame propagation velocity. This is done by determining the distance between corresponding points on the contours and divide with the time separation between the two images from which the contours have been determined. Corresponding points are here defined as a pair of points, one from each contour of a pair, marking the position of a certain point on the flame front at the time of image capture. A program was used to calculate the positions of a large number of corresponding points along the flame front by using the method of interpolation between a few corresponding points given as input. In figure 7(c) the contours from the images of figures 7(a) and (b) are shown together, illustrating the propagation of the flame front. In addition the $\times$-marks show the corresponding points given as user input for the velocity calculation.

4. Results

Three image pairs measured using the dual laser and ICCD setup and the engine running at close to stoichiometric conditions ($\lambda = 0.97$) are illustrated in figure 8. The first image of each pair was taken at -2 CAD and the second image was taken at -0.5 CAD. The time separation of 1.5 CAD

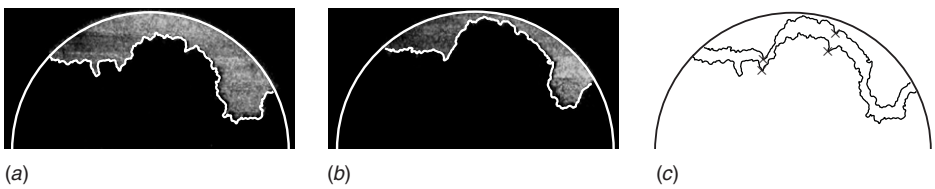

Figure 7. Formaldehyde LIF signal images detected at (a) -2 CAD and (b) -0.5 CAD. The identified contours have been superimposed on both images. (c) The two contours illustrated together. The corresponding points given as input for velocity calculation are indicated with $\times$-marks.

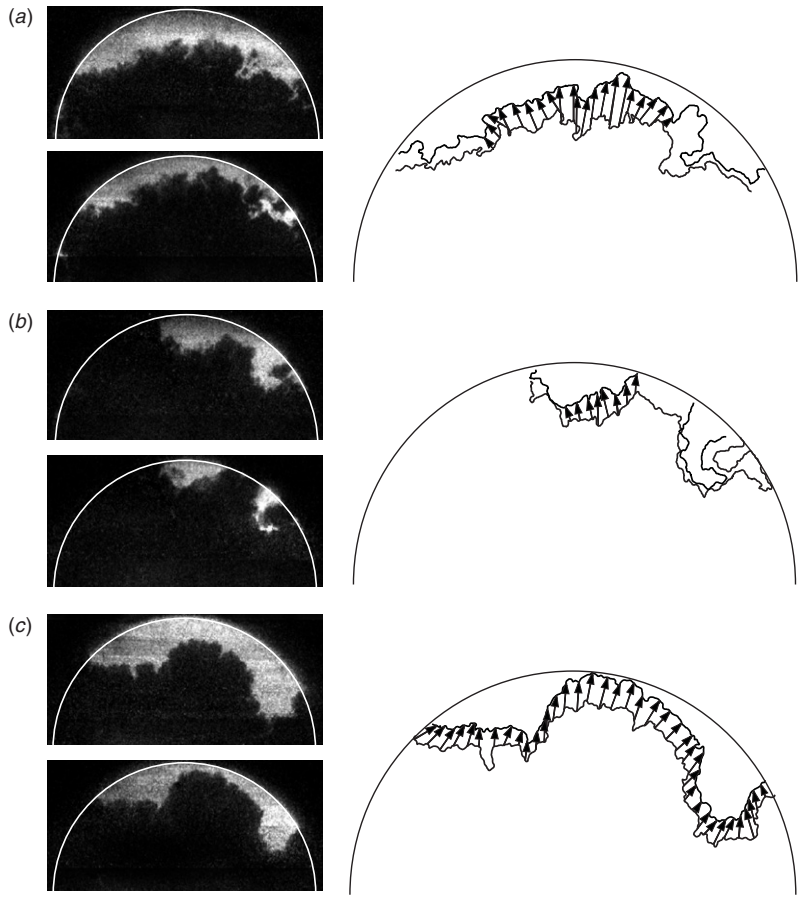

Figure 8. Three image pairs of formaldehyde LIF signals obtained in the engine shown together with the identified contours and velocity fields. The first image of each pair was taken at −2 CAD and the second at −0.5 CAD. Image pairs (*a*) and (*b*) were recorded with an intake temperature of $T = 30$ °C, whereas image pair (*c*) was recorded with an intake temperature of $T = 50$ °C.

corresponds to ∼210 μs, and was chosen as a compromise between higher accuracy in velocity estimation (for which a longer time separation is beneficial) and easier identification of corresponding contour points (for which a shorter time separation is beneficial).

Together with each image pair in figure 8 are also shown the identified contours and the calculated velocity field illustrated by arrows. The image pairs show some typical features encountered during the evaluation. For the image pair illustrated in figure 8(*a*) the signal detected at −2 CAD and at a pressure of 22 bar has three holes located in the right part of the signal area. In the image detected at −0.5 CAD and 25 bar it can be seen that the holes have expanded and the unburned mixture has been consumed from two directions. An indentation can also be seen in the region where the holes were located in the first image. The identified contour follows this indentation and interpreting the contour as a flame front will surely yield erroneous flame propagation results. The part of the contours with the large indentation must consequently be left out of the evaluation. In addition, it can be seen that the flame has propagated less in the far right part of the image, which may be due to the interaction with the fluid flow for this particular engine cycle.

In figure 8(*b*) a situation is shown where the propagation has resulted in two separate signal areas in the second image. The flame has propagated out of the piston view in part of the unburned region and therefore the flame propagation velocity cannot be evaluated along the entire contours. The registered pressure data for these images are 24 bar at −2 CAD and 27 bar at −0.5 CAD.

In contrast to figures 8(*a*) and (*b*) for which the intake temperature was 30 °C, the images shown in figure 8(*c*) were taken with an intake temperature of 50 °C, which has the consequence that the fuel–air mixture enters the first ignition stage earlier. With the elevated intake temperature, generally larger signal areas could be observed compared to images obtained with the lower intake temperature at the same crank angle degrees. For the images shown in figure 8(*c*) the pressures were 21 bar at −2 CAD and 24 bar at −0.5 CAD. With the exception of a small peninsula located in the left part of the image detected at −2 CAD, it is possible to evaluate the flame propagation velocity along the entire contours.

The evaluated flame propagation data presented in figure 8 resulted in mean speeds of (*a*) 21 m s^{-1}, (*b*) 14 m s^{-1}, and (*c*) 15 m s^{-1}. The values are reasonable compared to flame propagation values in a spark-ignition engine reported by Heywood [4].

The formaldehyde signal can be detected when the first ignition stage chemistry has been initiated. In our experiments this occurred in a limited crank angle interval around top dead centre. The initiation of combustion in the engine varies in time, crank angle degree, during operation. This is due to the increasing engine temperature during a measurement sequence as well as the inherent cycle-to-cycle variations of the engine. These factors determine the actual crank angle interval where the formaldehyde signal can be detected in a certain engine cycle. They also limit the number of image pairs from a measurement sequence that is useful for evaluation. Image pairs where one image shows no signal or signal with insufficient signal-to-noise ratio must obviously be discarded.

The number of data selected for flame propagation evaluation may also be further reduced during the evaluation procedure due to factors that will be described in the following text. The background subtraction procedure may in some cases give errors in the evaluated flame front contours, since the background images include reflections and fluorescence from the engine ceiling, and these additional signal contributions may vary during engine operation resulting in erroneous background compensation. The signal area of the compensated image will thus have a somewhat different appearance to that of the raw image at locations where the background signal is strong. The background contributions were suppressed by blackening the ceiling with soot before assembling the engine for measurements.

By studying the raw data together with the evaluated contours it was established that the use of profile compensation resulted in much better agreement between the boundaries of the signal areas and the identified contours. This has its origin in the binary image creation procedure, which will neglect regions of formaldehyde, where the signal is low due to low laser irradiance. The use of laser profile compensation circumvents this problem by enhancing the intensities in these regions before binary image creation.

The method presented here to estimate the flame propagation velocity is based on the assumption that the movement is two-dimensional since the measurements are made in a plane. Due to the pent-roof design of the engine, the third dimension cannot be neglected in the central parts of the combustion chamber. However, at the locations closer to the walls, the height of the chamber is lower and the flame front is believed to mainly evolve two-dimensionally. Three-dimensional effects may form holes and indentations in the contours of some images, mainly in areas located closer to the central region of the combustion chamber. The holes observed in the first image of figure 8(*a*) may be due to three-dimensional effects.

The program used to calculate corresponding points on the contours of an image pair relies on input data from the user. During the time interval separating the two images, the flame front has moved a few millimetres, generally towards the walls, but it has also to some degree changed shape. This obviously introduces an uncertainty in the identification of corresponding points on the contours and thereby also in the evaluated velocity. The uncertainty increases with increasing time separation since the flame front then changes its shape even more. As previously mentioned, this criterion gives an upper limit on the time separation that can be used.

Because of the issues described above, part of the data cannot be used for evaluation. However, problems imposed due to three-dimensional effects, inadequate background subtraction, etc mainly occur in isolated regions. For such cases these regions have been left unevaluated, whereas the signal areas in other regions have been used for velocity estimation. The images of figures 8(*a*) and (*b*) are examples where parts of the contours have been omitted in the flame propagation evaluation.

5. Discussion

Identifying unburned fuel–air mixture by nascent formaldehyde has also been performed in other investigations. Bäuerle *et al* performed measurements in the previously mentioned two-stroke research engine, and an identification of exothermic centres [9] was followed by a time-resolved study of the development of the centres [10]. The time-resolved experiments were performed using a setup consisting of two excimer lasers pumping a dye laser, resulting in two laser pulses at 353.2 nm. The tuneable laser makes it possible to use an efficient excitation line and is beneficial compared to the fixed Nd:YAG laser at 355 nm which excites at a less efficient transition [20]. The dye laser option, however, results in lower available pulse energy compared to the Nd:YAG laser. The low pulse energies ($\sim$2 mJ) used by Bäuerle *et al* [10] generally resulted in rather low signal-to-noise ratios of the presented images. Similar to our experiments Bäuerle *et al* observed a fluorescing end-gas region between the flame-front and the combustion chamber wall. The time separations between the laser pulses in [10] were typically tens of microseconds in order to study the fast development of exothermic centres.

The same engine geometry as presented in [9, 10] was also used by Schießl *et al* [14, 15] in experiments where two excimer lasers at 308 nm were used for excitation of different combustion intermediates occurring after the first ignition stage. The excitation at 308 nm was not species specific but also in this investigation a fluorescing region of unburned mixture could be observed as well as exothermic centres. The high pulse energy available in those experiments was beneficial to the image signal-to-noise ratio. The appearance of the flame front in the presented images resembles the results obtained in our experiments. In [14], Schießl *et al* present pairs of images detected with different time separations. Similar to the results in [10], time separations of the order of tens of microseconds resulted in no apparent movement of the flame front, whereas a growth of the exothermic centres could be traced. For separations of hundreds of microseconds also a movement of the flame front could be observed, in agreement with our observations.

The method presented in this paper for flame propagation measurements is based on the assumption that the boundary of the formaldehyde LIF signal marks the flame front. However, the formaldehyde indicates regions of cool-flame chemistry, which not necessarily must indicate the total unburned region, thus introducing an uncertainty in the determination of the flame front. Therefore it is of interest to compare the formaldehyde signal with a well-known method used for fuel visualization, such as fluorescence from a tracer species.

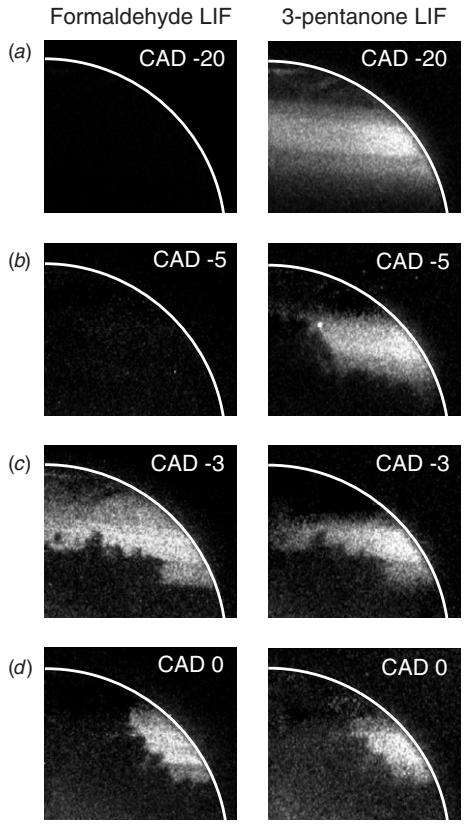

Figure 9. Simultaneous formaldehyde and 3-pentanone LIF images obtained at different crank angles; (*a*) −20 CAD, (*b*) −5 CAD, (*c*) −3 CAD, (*d*) 0 CAD. It should be noted that the four pairs were recorded in different engine cycles.

A suitable tracer species for iso-octane is 3-pentanone [22, 23], and LIF from this tracer has been measured simultaneously with LIF from formaldehyde by Graf *et al* [12]. They performed measurements in an engine operated in a controlled auto-ignition mode with a geometry similar to that of our engine.

Our experimental setup was thus re-arranged for quasi-simultaneous measurements where one Nd:YAG laser fired a laser pulse at 355 nm (exciting nascent formaldehyde), and one Nd:YAG laser fired 0.02 crank angles later at 266 nm (exciting added 3-pentanone). Four image pairs showing the right half of the measurement area depicted in figure 2 and detected at different crank angles are shown in figure 9. These images have not been corrected for non-uniformities in the spatial distribution of laser intensity and, as previously mentioned, the laser sheet widths were set to ∼2 cm in order to increase the power densities and hence the signal-to-noise ratio.

Figure 9(*a*) shows two images detected at −20 CAD and an engine pressure of 8 bar. The formaldehyde LIF image (left) shows no signal at this crank angle, which is to be expected since the fuel–air mixture has not entered the first ignition stage at this crank angle and no cool-flame species have been created. The detected 3-pentanone LIF image showed fluorescence from the tracer that covered the entire length of the sheet, of which only the right half is shown in the fuel tracer image of figure 9(*a*). The spark has been ignited at −30 CAD, but so far the air–fuel mixture in the sheet has not been consumed by the propagating flame since the probe volume is located in the lower part of the combustion chamber, whereas the spark plug is located in the upper part. Figure 9(*b*) shows an image pair taken at −5 CAD and 17 bar. Again no signal from formaldehyde can be observed, but in the fuel tracer image it can be seen from the lack of signal in the left part of the figure that part of the mixture has burned. In figure 9(*c*) an image pair is shown that has been detected at −3 CAD and 24 bar. In this case signals can be seen in both images. The boundaries between the burned and unburned regions show similar shape and position and even small details can be compared and identified. Because of the separate laser beam paths, the signal from the laser sheet edges may differ between the images. This is evident when comparing the signals in the upper part of the images in figure 9(*c*). In figure 9(*d*) an image pair detected at 0 CAD and 29 bar shows a similar situation to that of figure 9(*c*), with boundaries of similar position and shape appearing in both images. Also in this case it is possible to identify small details that appear in both images. The signal areas of these images are smaller than the ones in figure 9(*c*) since more of the air–fuel mixture has burned. For the images detected at −3 and 0 CAD (figures 9(*c*) and (*d*)) both the fuel tracer LIF and the formaldehyde LIF are good indicators of the unburned mixture. The signal-to-noise ratio was higher for the formaldehyde images than for the fuel tracer images and a comparison between the signal intensities gave a ratio of ∼2 for similar pulse energies under the given experimental conditions.

The similar appearance of the signals from the two techniques presented in figures 9(*c*) and (*d*) could be observed for all measured cycles where the signal-to-noise ratio of both images in a pair was sufficiently high for successful image evaluation. From this the conclusion was drawn that in the present case both alternatives could be used for visualization of unburned regions. However, the techniques have different advantages and disadvantages. The fuel tracer must be added to the fuel and may interfere with the combustion process, whereas the formaldehyde is formed naturally. However, the fuel tracer can be detected from mixture intake up to combustion, whereas formaldehyde is only present at conditions where temperature and pressure are high enough for the cool-flame chemistry to be initiated. This limits the formaldehyde detection spatially to the end-gas region of the engine and temporally to a certain crank angle interval, in our case between approximately −5 and +5 CAD. It should also be noted that the formaldehyde alternative requires a fuel that has two-stage ignition chemistry. When present, the formaldehyde results in strong LIF signals yielding single-shot images of good quality and proved in our case to be a better choice than the fuel tracer.

6. Summary

Experimental investigations of flame propagation have been performed in a spark-ignition engine using laser-induced fluorescence of cool-flame species, among these formaldehyde. The two-dimensional visualization experiments were based on a setup with two synchronized Nd:YAG lasers at 355 nm with an arbitrarily set delay between the pulses, and two ICCD cameras each synchronized with

one of the lasers. Flame propagation velocities were evaluated from the pairs of formaldehyde LIF images following a scheme with creation of binary images from which the signal contours could be identified. Since the identified contours are indicators of the location of the flame front at certain time positions, the velocity vectors could be determined along the flame front. Mean speeds in the range of 10–20 m s^{-1} were generally obtained. The characteristics of the method using LIF of formaldehyde have been discussed and given the right circumstances, the method has shown to be useful for flame propagation velocity estimation.

Additionally the formaldehyde LIF was compared with fuel tracer LIF as an indicator of the unburned mixture. This was performed in quasi-simultaneous measurements, where the formaldehyde was excited using 355 nm and 3-pentanone was excited at 266 nm. The measurements showed that both methods traced the same areas, i.e. the unburned fuel–air mixture, and that the identified contours indicate the boundary between unburned and burned mixtures.

One merit of the presented method for two-dimensional velocity estimation is that formaldehyde is a nascent species formed during the first-ignition stage of many hydrocarbons, thus making it unnecessary to add a fuel tracer. However, it should be noted that not all hydrocarbons form cool-flame species and thereby formaldehyde. Moreover, the first ignition stage is not entered until the unburned gas mixture has reached a temperature of around 650–700 K [4], thus the flame propagation process cannot be followed in the initial phase. Further merits of the formaldehyde method are that the use of Nd:YAG lasers at 355 nm for the excitation is relatively simple, yielding high pulse energies and relatively strong laser-induced fluorescence signals.

Acknowledgments

The support from the staff at the Department of Thermo and Fluid Dynamics at Chalmers University of Technology is gratefully acknowledged, especially Allan Sognell. The authors also acknowledge the support from Mattias Richter concerning the initial evaluation of the images and Thomas Metz for providing the formaldehyde cell spectra. The financial support from the Swedish National Energy Administration is gratefully acknowledged.

References

[1] Eckbreth A C 1996 *Laser Diagnostics for Combustion Temperature and Species* 2nd edn (London: Gordon and Breach)

[2] Kohse-Höinghaus K and Jeffries J B (ed) 2002 *Applied Combustion Diagnostics* (New York: Taylor and Francis)

[3] Daily J W 1997 Laser-induced fluorescence spectroscopy in flames *Prog. Energy Combust. Sci.* **23** 133–99

[4] Heywood J B 1988 *Internal Combustion Engine Fundamentals* (New York: McGraw-Hill)

[5] Harrington J E and Smyth K C 1993 Laser-induced fluorescence measurements of formaldehyde in a methane/air diffusion flame *Chem. Phys. Lett.* **202** 196–202

[6] Burkert A, Grebner D, Müller D, Tribel W and König J 2000 Single-shot imaging of formaldehyde in hydrocarbon flames by XeF excimer laser-induced fluorescence *Proc. Combust. Inst.* **28** 1655–61

[7] Böckle S, Kazenwadel J, Kunzelmann T, Shin D-I and Schulz C 2000 Single-shot laser-induced fluorescence imaging of formaldehyde with XeF excimer excitation *Appl. Phys.* B **70** 733–5

[8] Shin D I, Dreier T and Wolfrum J 2001 Spatially resolved absolute concentration and fluorescence-lifetime determination of H_2CO in atmospheric-pressure CH_4/air flames *Appl. Phys.* B **72** 257–61

[9] Bäuerle B, Hoffmann F, Behrendt F and Warnatz J 1994 Detection of hot spots in the endgas of an internal combustion engine using two-dimensional LIF of formaldehyde *Proc. Combust. Inst.* **25** 135–41

[10] Bäuerle B, Behrendt F and Warnatz J 1996 Time-resolved investigation of hot spots in the end gas of an S.I. engine by means of 2-d double pulse LIF of formaldehyde *Proc. Combust. Inst.* **26** 2619–26

[11] Schießl R, Pixner P, Dreizler A and Maas U 1999 Formaldehyde formation in the endgas of Otto-engines: numerical simulations and quantitative concentration measurements *Combust. Sci. Tech.* **149** 339–60

[12] Graf N, Gronki J, Schulz C, Baritaud T, Cherel J, Puret P and Lavy J 2001 In-cylinder combustion visualization in an auto-igniting gasoline engine using fuel tracer- and formaldehyde-LIF imaging SAE 2001-01-1924

[13] Collin R, Nygren J, Richter M, Aldén M, Hildingsson L and Johansson B 2003 Simultaneous OH- and formaldehyde-LIF measurements in an HCCI engine *SAE Paper* 2003-01-3218

[14] Schießl R, Dreizler A, Maas U, Grant A J and Ewart P 2001 Double-pulse imaging of self-ignition centers in an SI-engine *SAE Paper* 2001-01-1925

[15] Schießl R and Maas U 2003 Analysis of endgas temperature fluctuations in an SI engine by laser-induced fluorescence *Combust. Flame* **133** 19–27

[16] Dieke G H and Kistiakowsky G B 1934 The structure of the ultraviolet absorption spectrum of formaldehyde: 1 *Phys. Rev.* **45** 4–28

[17] Miller R G and Lee E K C 1978 Single vibronic level photochemistry of formaldehydes in the $\tilde{A}^1A_2$ state: radiative and non-radiative processes in the H_2CO, HDCO and D_2CO *J. Chem. Phys.* **68** 4448–64

[18] Clouthier D J and Ramsay D A 1983 The spectroscopy of formaldehyde and thio-formaldehyde *Ann. Rev. Phys. Chem.* **34** 31–58

[19] Strickler S J and Barnhart R J 1982 Absolute vibronic intensities in the $^1A_2 \leftarrow {}^1A_1$ absorption spectrum of formaldehyde *J. Phys. Chem.* **86** 448–55

[20] Brackmann C, Nygren J, Bai X, Li Z, Bladh H, Axelsson B, Denbratt I, Koopmans L, Bengtsson P-E and Aldén M 2003 Laser-induced fluorescence of formaldehyde in combustion using third harmonic Nd:YAG laser excitation *Spectrochim. Acta* A **59** 3347–56

[21] Metz T, Bai X, Ossler F and Aldén M 2004 Fluorescence lifetimes of formaldehyde (H_2CO) in the $A^1A_2 \leftarrow X^1A_1$ band system at elevated temperatures and pressures *Spectrochim. Acta* A **60** 1043–53

[22] Zhao H and Ladommatos N 1998 Optical diagnostics for in-cylinder mixture formation measurements in IC engines *Prog. Energy Combust. Sci.* **24** 297–336

[23] Neij H, Johansson B and M 1994 Development and demonstration of 2D-LIF for studies of mixture preparation in SI engines *Combust. Flame* **99** 449–57